

# Influence on lacustrine source rock by hydrothermal fluid: a case study of the Chang 7 oil shale, southern Ordos Basin

Delu Li<sup>1</sup> · Rongxi Li<sup>1</sup> · Zengwu Zhu<sup>2</sup> · Xiaoli Wu<sup>1</sup> ·  
Futian Liu<sup>1</sup> · Bangsheng Zhao<sup>1</sup> · Baoping Wang<sup>3</sup>

Received: 25 April 2017 / Revised: 2 June 2017 / Accepted: 3 July 2017 / Published online: 10 July 2017  
© Science Press, Institute of Geochemistry, CAS and Springer-Verlag GmbH Germany 2017

**Abstract** Hydrothermal fluid activity during sedimentation of the Triassic Yanchang Formation in the Ordos Basin and the impact of said activity on formation and preservation conditions of source rocks have received little attention. Oil yield, major element, trace element, rare earth element, and total sulfur (TS) data from the oil shale within the Yanchang are here presented and discussed in the context of hydrothermal influence. Oil shale samples returned relatively high total organic carbon (TOC), in the range of 4.69%–25.48%. A high correlation between TS and TOC suggests TS in the oil shale is dominated by organic sulfur and affected by organic matter. The low Al/Si ratio of oil shale samples implies quartz is a major mineralogical component. Si/(Si + Al + Fe) values suggest close proximity of the oil shale to a terrigenous source.  $\delta\text{Eu}$ ; Fe versus Mn versus  $(\text{Cu} + \text{Co} + \text{Ni}) \times 10$ ; and  $\text{SiO}_2/(\text{K}_2\text{O} + \text{Na}_2\text{O})$  versus  $\text{MnO}/\text{TiO}_2$ , Fe/Ti, and  $(\text{Fe} + \text{Mn})/\text{Ti}$  are evidence of hydrothermal fluid activity during oil shale sedimentation, and  $\delta\text{U}$  and U/Th of the oil shale indicate reducing conditions. The Sr/Ba of oil shale samples suggests fresh-water deposition. The high correlations of Fe/Ti and  $(\text{Fe} + \text{Mn})/\text{Ti}$  with  $\delta\text{U}$ , U/Th, and TS demonstrate that hydrothermal fluid activity promotes reducing conditions. Sr/Ba ratios had low correlation with Fe/Ti and  $(\text{Fe} + \text{Mn})/\text{Ti}$ , implying that hydrothermal fluid activity had little impact on paleosalinity. Fe/Ti,  $(\text{Fe} + \text{Mn})/\text{Ti}$ ,  $\delta\text{U}$ , U/Th, and Cu + Pb + Zn all exhibited

high positive correlation coefficients with TOC in oil shale samples, suggesting that more intense hydrothermal fluid activity improves conditions in favor of formation and preservation of organic matter.

**Keywords** Hydrothermal fluid activity · Lacustrine source rock · Element geochemistry · Chang 7 · Ordos Basin

## 1 Introduction

The study of hydrothermal fluid activity started in the 1960s and has been a research hotspot of fluid metallogenesis (Bischoff 1969; Zeng et al. 2015). Previous research has suggested that hydrothermal fluid activity could transport massive thermal energy, chemical energy, and metallogenetic materials, making it one of the most important mineral-forming geologic processes (Zhang et al. 2010). Research of hydrothermal fluid activity has focused mainly on metallic ore in the marine environment (Qi et al. 2015; Zeng et al. 2015) and studies of hydrocarbon resources in the context of hydrothermal activity are primarily focused on marine siliceous shale, carbonaceous shale, and dolomite of the Cambrian and Silurian Niutitang and Longmaxi Formations in southern China (Sun et al. 2003, 2004; Chen et al. 2004; Chen and Sun 2004; Jia et al. 2016). Post-Permian source rocks with a lacustrine sedimentary environment affected by hydrothermal activity are in northern China (Liu et al. 2010; Zhang et al. 2010). The formation of these source rocks is closely associated with hydrothermal fluid activity (Xie et al. 2015; Chu et al. 2016; He et al. 2016, 2017; Jia et al. 2016). Nutrients and elements transported in hydrothermal fluids affect organic matter, but the impact is disputed. Some scholars argue hydrothermal activity increases organic matter

✉ Rongxi Li  
Rongxi99@163.com

<sup>1</sup> School of Earth Sciences and Resources, Chang'an University, Xi'an 710054, China

<sup>2</sup> Shaanxi Center of Geological Survey, Xi'an 710068, China

<sup>3</sup> Yanchang Oilfield Co., Ltd, Yan'an 716000, China

concentration (Zhang et al. 2010; He et al. 2016), while others suggest it can render the environment inhospitable for the formation of organic matter (Xie et al. 2015; Chu et al. 2016).

The Triassic Yanchang Formation in the Ordos Basin went through four periods of hydrothermal fluid activity, of which Chang 7 represents the peak in scale and intensity. The oil shale from Chang 7 is the superior Triassic source rock. The formation of the oil shale is considered to have occurred in a deep lake environment. But some evidence, such as micro- and nano-fossils (Zhang et al. 2011), tuff (Qiu et al. 2009, 2011), and high-gamma sandstone (Liu et al. 2013), suggest the presence of hydrothermal activity during oil shale sedimentation. Due to its high total organic carbon (TOC), the viewpoint that hydrothermal fluid activity has a positive effect on the formation of oil shale is widely accepted (Lai et al. 2010; Zhang et al. 2010; Wang et al. 2014a, b). However, relevant evidence remains in the qualitative stage, there being insufficient quantitative data.

In this study, considering the high organic matter in oil shale relative to other source rocks, along with advantages of research regulations, we selected oil shale samples in the southern Ordos Basin. TOC of oil shale samples was

calculated based on the relationship of TOC with oil yield. Then, elemental characteristics of oil shale samples were studied to ascertain hydrothermal fluid activity. Following correlation analyses of element ratios, calculated values, and TOC, the influence of hydrothermal fluid activity on organic matter is discussed.

## 2 Geologic setting

Located in a structurally bound site of central China, the Ordos Basin is one of the country's main hydrocarbon basins. It consists of six first-order tectonic units: the Weibei Uplift, Yishan Slope, Yimeng Uplift, Jinxi Flexure Zone, Tianhuan Depression, and Western Thrusted Zone (Fig. 1a) and is the end product of a tectonic orogeny involving the Pacific Plate and Tethyan oceanic crust following Indosinian movement over Paleoproterozoic crystalline basement (Wang 2011; Li et al. 2016). By the Early Triassic, sedimentary facies were primarily fluvial and swamp facies (He 2003; He et al. 2016). Subsequently, the basin gradually developed lacustrine facies in the Yanchang Formation of the Upper Triassic (Wang 2011).

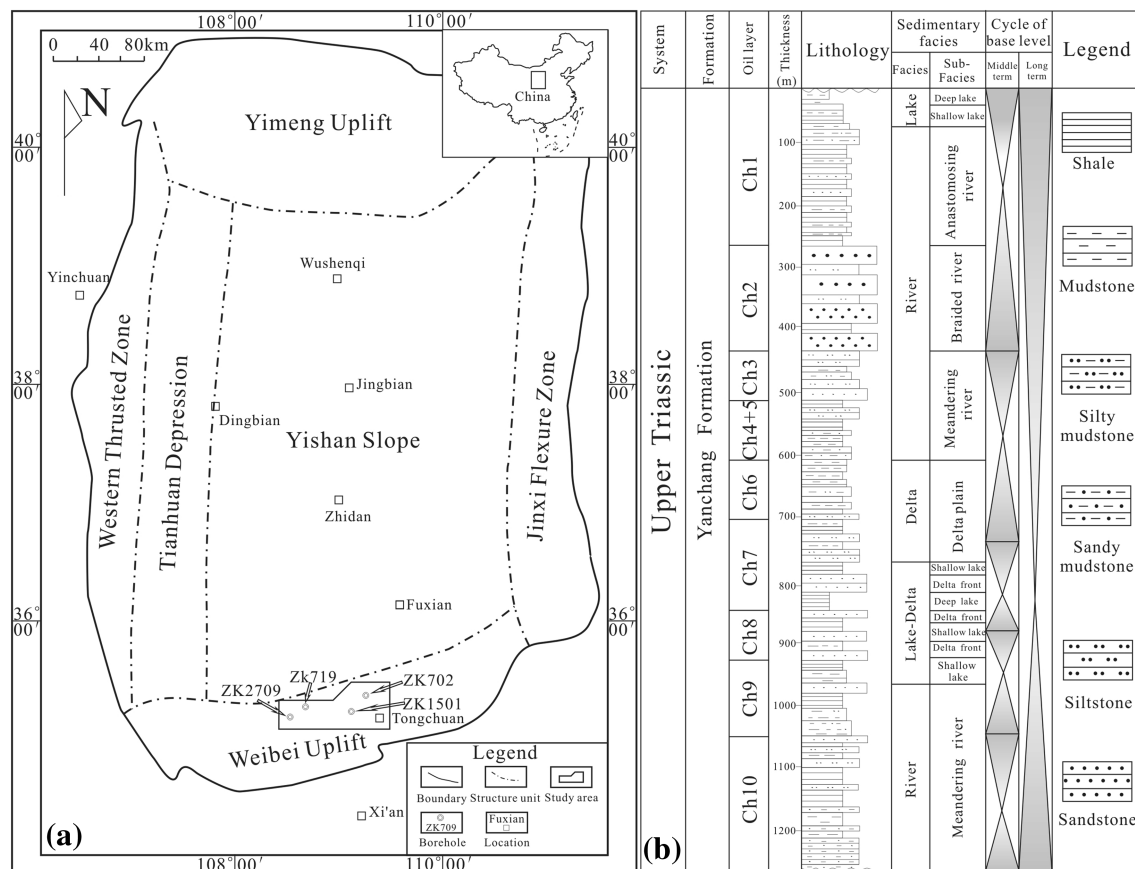


**Fig. 1** **a** The geological map of Ordos Basin and locations of studied boreholes and **b** stratigraphic column of Upper Triassic Yanchang Formation (modified after Qiu et al. 2014). Ch = Chang, the same hereinafter

Toward the end of the Triassic, the lake gradually dried out (He 2003). According to sedimentary cycles, the Yanchang Formation has been divided into ten oil layers (Chang 10 to Chang 1 from bottom to top) as seen in the Changqing Oilfield (Yang et al. 1992), which shows a transgressive-regressive lacustrine cycle (Fig. 1b) (Qiu et al. 2014). During the deposition of Chang 7, the lake reached its largest size (Wu et al. 2004), forming a superior oil shale known as the “Zhangjitan Shale,” under a climate that was mainly warm and humid (Zhang et al. 2011). The bottom of the Chang 7 oil layer is composed of oil shale, mudstone, siltstone, and tuff.

### 3 Samples and analytical methods

Twenty-one samples collected from four boreholes in the oil shale section were analyzed for oil yield, major elements, rare earth elements (REEs), and total sulfur (TS). Samples were 70 mm in diameter and 30 cm long and were stored separately in plastic bags until tested to minimize contamination and oxidation. Sampling locations and rock assemblages are shown in Fig. 2.

For oil yield analysis, samples were ground to particle size <3 mm, then 50 g was enclosed in aluminum retort and heated to 520 °C under air-free conditions. The analytical method was low temperature carbonization and the procedures followed the Chinese standard method SH/T 0508-1992 (1992). The analytical uncertainty was within 5%.

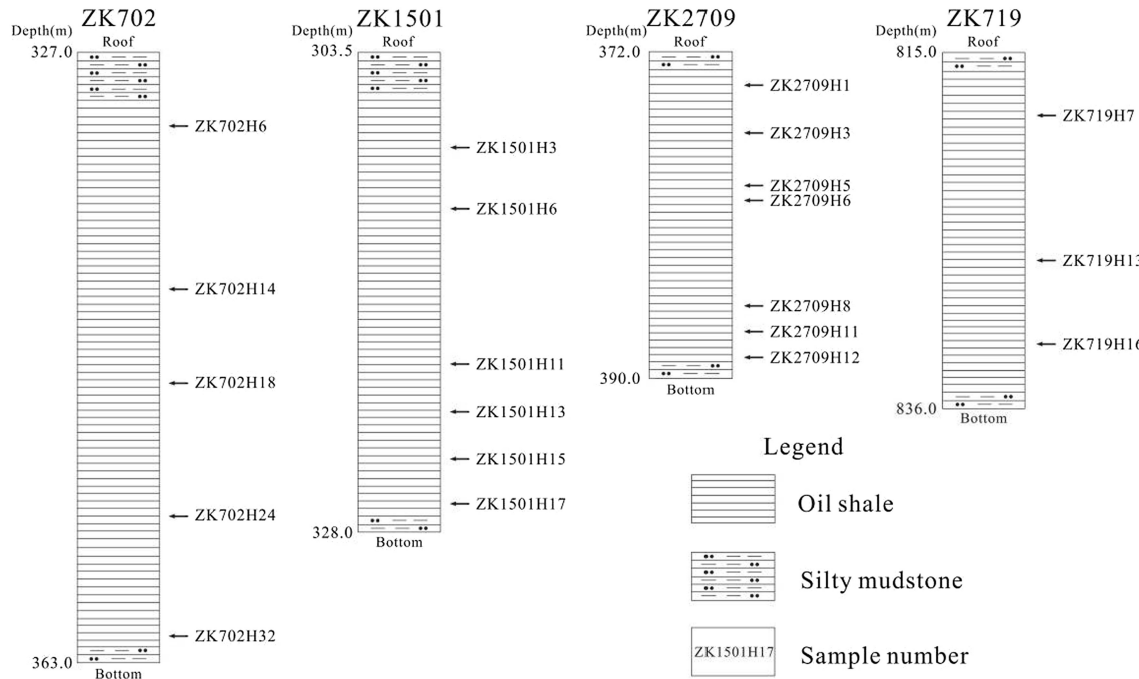


**Fig. 2** Oil shale sections from the bottom of Chang 7 formation, showing sampling locations

For major elements analysis, samples were crushed and ground to less than 200 mesh for X-ray fluorescence spectrometry (XRF) with AA-6800 atomic absorption spectroscopy and UV-2600 ultraviolet-visible spectrophotometer. The analytical procedures followed Chinese National Standard GB/T14506.1 ~ 14-2010 (2010). The analytical uncertainty was usually within 5%.

REE and trace element concentrations were determined with a Perkin Elmer SciexElan 6000 inductively-coupled plasma–mass spectrometer (ICP-MS), by the method of Chinese National Standard GB/T14506.30-2010 (2010). The analytical precision was generally within 5%.

The samples for TS test were ground to <100 µm, and then heated in a pipe furnace to 1250 ± 20 °C with fluxing agent of cupric oxide powder. The analysis method followed Chinese National Standard GB/T 6730.17-2014 (2014).

Oil yield analysis was conducted at Shaanxi Coal Geological Laboratory Co., Ltd. Major element, trace element, and REE concentrations and TS were analyzed at Analytical Center, No. 203, Research Institute of Nuclear Industry.

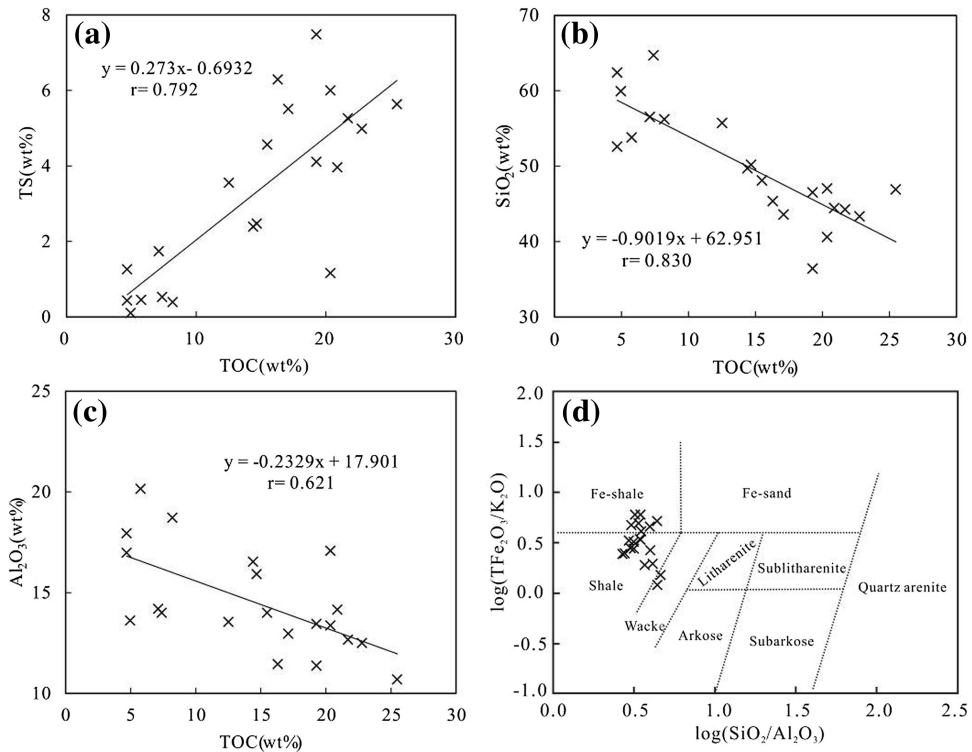
## 4 Results

### 4.1 Oil yield, total organic carbon, and total sulfur

Oil shale samples had high oil yield (1.40 wt%–9.10 wt%, averaging 5.01 wt%), indicating relatively high quality (Table 1). Sun et al. (2011) discovered that oil yield of oil shales in the southern Ordos Basin is related to TOC

**Table 1** Oil yield, total organic carbon (TOC), total sulfur (TS), major element concentrations, Al/Si and Si/(Si + Al + Fe) of oil shale samples (oil yield, TOC, TS, and major elements in wt%)

Sample no.	Oilyield	TOC	TS	SiO <sub>2</sub>	Al <sub>2</sub> O <sub>3</sub>	TFe <sub>2</sub> O <sub>3</sub>	MgO	CaO	Na <sub>2</sub> O	K <sub>2</sub> O	P <sub>2</sub> O <sub>5</sub>	MnO	Al/Si	Si/(Si + Al + Fe)
ZK702H6	4.30	12.52	3.55	55.73	13.54	6.95	0.75	0.42	0.98	3.61	0.24	0.09	0.37	0.62
ZK702H14	7.20	20.35	6.00	40.61	13.37	10.52	0.97	0.97	0.91	2.25	0.28	0.05	0.50	0.50
ZK702H18	9.10	25.48	5.63	46.90	10.69	9.48	0.86	1.61	1.30	1.85	0.45	0.06	0.34	0.57
ZK702H24	8.10	22.78	4.98	43.33	12.50	8.85	0.98	1.67	1.49	1.49	0.35	0.07	0.44	0.54
ZK702H32	7.70	21.70	5.26	44.26	12.66	9.62	0.93	1.25	1.00	2.37	0.29	0.09	0.43	0.54
ZK1501H3	5.70	16.30	6.29	45.36	11.45	9.57	1.06	1.62	1.45	2.12	0.36	0.11	0.38	0.55
ZK1501H6	6.80	19.27	7.48	36.42	11.37	11.27	1.45	2.19	0.74	1.90	0.26	0.08	0.47	0.48
ZK1501H11	6.00	17.11	5.51	43.58	12.96	9.87	1.16	2.36	1.43	2.03	0.41	0.21	0.45	0.53
ZK1501H13	2.30	7.12	1.74	56.52	14.20	5.48	2.31	3.48	1.92	2.09	0.23	0.10	0.38	0.64
ZK1501H15	5.40	15.49	4.56	48.09	14.00	7.97	1.22	1.98	1.30	2.36	0.46	0.25	0.44	0.56
ZK1501H17	1.50	4.96	0.10	59.95	13.61	4.86	2.13	3.59	2.25	4.11	0.15	0.13	0.34	0.66
ZK2709H1	1.80	5.77	0.45	53.80	20.15	7.28	2.08	0.94	1.17	3.02	0.23	0.23	0.57	0.54
ZK2709H3	7.40	20.89	3.96	44.44	14.15	8.03	1.71	1.59	1.29	2.53	0.39	0.19	0.48	0.54
ZK2709H5	2.40	7.39	0.53	64.70	14.00	3.61	1.19	1.24	1.73	2.43	0.12	0.14	0.33	0.69
ZK2709H6	6.80	19.27	4.11	46.51	13.44	7.46	1.76	2.09	1.39	2.23	0.38	0.19	0.44	0.57
ZK2709H8	5.10	14.68	2.47	50.17	15.92	7.61	2.01	1.17	1.14	2.80	0.27	0.16	0.48	0.56
ZK2709H11	5.00	14.41	2.39	49.72	16.53	7.54	2.06	1.02	1.03	2.74	0.23	0.13	0.50	0.55
ZK2709H12	1.40	4.69	0.43	62.40	16.97	5.80	2.09	0.39	2.05	3.10	0.13	0.06	0.41	0.63
ZK719H7	1.40	4.69	1.26	52.60	17.95	7.16	2.39	1.39	0.78	2.18	0.15	0.14	0.52	0.56
ZK719H13	7.20	20.35	1.16	47.03	17.07	6.21	1.74	0.73	0.76	2.54	0.24	0.15	0.55	0.55
ZK719H16	2.70	8.20	0.39	56.23	18.72	6.14	2.08	1.92	0.82	2.22	0.14	0.09	0.50	0.58
Average	5.01	14.45	3.25	49.92	14.54	7.68	1.57	1.60	1.28	2.47	0.27	0.13	0.44	0.57

**Fig. 3** a–c Correlation diagrams of TOC with TS, SiO<sub>2</sub> and Al<sub>2</sub>O<sub>3</sub> concentration of oil shale samples (d) lithology classification of oil shale samples and the base map is from He et al. (2016)

**Table 2** Rare earth elements and related parameters of oil shale samples (rare earth elements in ppm)

Sample no.	La	Ce	Pr	Nd	Sm	Eu	Gd	Tb	Dy	Ho	Er	Tm	Yb	Lu	$\Sigma$ LREE	$\Sigma$ HREE	$\Sigma$ REE	L/H	$\delta$ Eu	$\delta$ Ce
ZK702H6	42.70	82.30	8.81	38.20	7.56	1.14	6.70	1.24	5.91	1.57	3.84	0.76	4.81	0.82	180.71	25.65	206.36	7.05	0.70	0.92
ZK702H14	34.00	63.50	6.71	28.50	5.07	1.29	4.57	0.74	3.31	0.89	2.04	0.37	2.50	0.37	139.07	14.79	153.86	9.40	1.18	0.91
ZK702H18	32.70	61.60	6.64	29.20	5.22	1.39	5.11	0.86	3.85	1.01	2.34	0.42	2.73	0.42	136.75	16.74	153.49	8.17	1.18	0.91
ZK702H24	30.20	55.70	6.06	26.80	5.10	1.52	4.66	0.78	3.66	0.92	2.09	0.40	2.38	0.35	125.38	15.24	140.62	8.23	1.37	0.89
ZK702H32	35.60	66.90	7.19	30.00	5.33	1.36	4.97	0.78	3.16	0.84	1.97	0.32	2.16	0.36	146.38	14.56	160.94	10.05	1.16	0.91
ZK1501H3	33.20	62.20	6.43	26.90	5.10	1.13	4.46	0.76	3.28	0.85	1.88	0.36	2.27	0.37	134.96	14.23	149.19	9.48	1.04	0.92
ZK1501H6	33.10	60.50	6.45	27.30	5.27	1.26	4.76	0.76	3.60	0.95	2.14	0.40	2.70	0.40	133.88	15.71	149.59	8.52	1.10	0.90
ZK1501H11	29.90	55.80	5.98	26.00	4.77	1.40	4.69	0.72	3.33	0.87	2.02	0.38	2.27	0.38	123.85	14.66	138.51	8.45	1.30	0.90
ZK1501H13	37.60	68.80	6.88	27.60	4.95	1.38	4.51	0.74	3.16	0.88	1.97	0.37	2.48	0.40	147.21	14.51	161.72	10.15	1.28	0.92
ZK1501H15	40.40	75.80	8.19	34.90	6.44	1.74	5.74	0.99	4.37	1.21	2.61	0.54	3.19	0.50	167.47	19.15	186.62	8.75	1.26	0.90
ZK1501H17	35.80	67.00	7.03	28.90	5.00	1.54	4.63	0.66	2.82	0.73	1.68	0.31	2.06	0.30	145.27	13.19	158.46	11.01	1.41	0.91
ZK2709H1	49.70	100.00	9.55	39.80	7.30	1.52	6.46	1.02	4.89	1.05	3.09	0.52	3.28	0.48	207.87	20.79	228.66	10.00	0.97	0.99
ZK2709H3	39.30	76.00	7.23	31.00	5.41	1.29	5.52	0.80	4.41	1.06	2.54	0.40	2.52	0.37	160.23	17.62	177.85	9.09	1.03	0.97
ZK2709H5	39.80	77.80	7.50	30.00	5.46	1.04	5.18	0.90	4.32	0.89	2.66	0.43	2.54	0.37	161.60	17.29	178.89	9.35	0.86	0.97
ZK2709H6	35.40	66.50	6.59	27.80	5.14	1.19	4.65	0.78	3.56	0.90	2.46	0.34	2.31	0.36	142.62	15.36	157.98	9.29	1.07	0.94
ZK2709H8	40.90	80.50	7.75	32.90	5.61	1.36	4.93	0.79	3.59	0.85	2.39	0.36	2.26	0.39	169.02	15.56	184.58	10.86	1.14	0.98
ZK2709H11	43.30	80.50	7.66	33.20	6.16	1.51	5.67	0.84	3.95	0.89	2.35	0.40	2.38	0.35	172.33	16.83	189.16	10.24	1.12	0.95
ZK2709H12	36.70	75.40	6.97	29.60	5.30	1.15	4.98	0.82	4.06	1.01	2.62	0.42	2.34	0.38	155.12	16.63	171.75	9.33	0.98	1.02
ZK719H7	46.40	91.50	8.70	35.70	6.29	1.42	5.84	0.85	3.77	0.95	2.51	0.37	2.45	0.42	190.01	17.16	207.17	11.07	1.03	0.98
ZK719H13	48.00	94.80	9.08	37.80	6.47	1.46	5.54	0.85	3.72	1.01	2.51	0.41	2.44	0.39	197.61	16.87	214.48	11.71	1.07	0.98
ZK719H16	47.70	94.10	8.96	37.20	6.00	1.47	5.48	0.88	4.09	0.99	2.73	0.45	2.58	0.40	195.43	17.60	213.03	11.10	1.13	0.98
Average	38.69	74.15	7.45	31.40	5.66	1.36	5.19	0.84	3.85	0.97	2.40	0.42	2.60	0.41	158.70	16.67	175.38	9.59	1.11	0.94
NASC <sup>a</sup>	32.00	73.00	7.90	33.00	5.70	1.24	5.20	0.85	5.80	1.04	3.40	0.50	3.10	0.48	152.84	20.37	173.21	7.50	/	/

<sup>a</sup> Data cited are from Taylor and McLennan (1985)

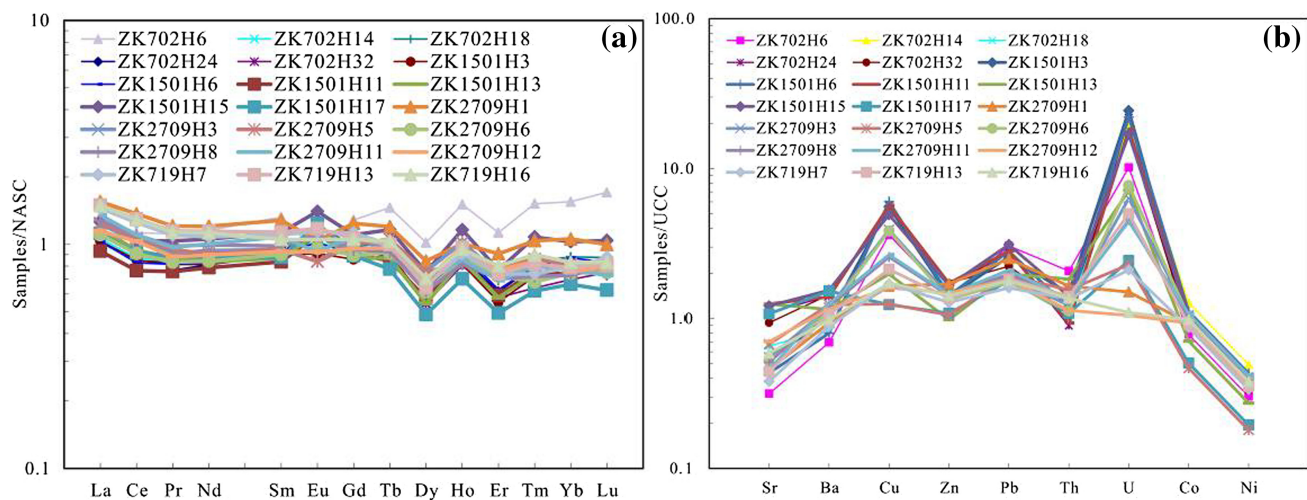


**Fig. 4** **a** REEs distribution pattern and **b** spider diagram of trace elements of oil shale samples

( $r = 0.894$ ) by:  $T = 2.7 \times \omega + 0.907$  where  $T$  and  $\omega$  represent TOC (wt%) and oil yield (wt%), respectively. TOC of oil shale samples was thus calculated to range from 4.69 wt% to 25.48 wt%, with an average of 14.45 wt% (Table 1). TS includes organic and inorganic sulfur and its content was relatively high with a range of 0.10 wt%–7.48 wt% (Table 1). Positive correlation ( $r = 0.792$ ) between TOC and TS content shows that sulfur in oil shale samples is mainly organic sulfur, strongly influenced by organic matter (Fig. 3a).

## 4.2 Element characteristics

### 4.2.1 Major element characteristics

$\text{SiO}_2$ ,  $\text{Al}_2\text{O}_3$ , and  $\text{TiFe}_2\text{O}_3$  (total iron) were the most abundant three elements in oil shale samples (36.42%–64.70%, 10.69%–20.15%, and 3.61%–11.27%, respectively) (Table 1). Other major elements were detected at concentrations of no more than 5%. The Al/Si ratio can be used to determine minerals in oil shale; the ratio gradually declines as the content of quartz increases (Fu et al. 2010a, b). The Al/Si ratios of oil shale samples were very low (0.33–0.57) (Table 1), implying domination by quartz, which is in accordance with previous X-ray diffraction analysis (Qiu et al. 2015).  $\text{Si}/(\text{Si} + \text{Al} + \text{Fe})$  can provide information on distance from terrigenous provenance, decreasing with increasing distance (Chen and Sun 2004). The  $\text{Si}/(\text{Si} + \text{Al} + \text{Fe})$  ratio of oil shale samples ranged from 0.48 to 0.69, suggesting that the oil shale was deposited not far away from a terrigenous provenance. Terrigenous matter input can dilute organic matter, leading to negative correlation between TOC and  $\text{Al}_2\text{O}_3$  concentration (Fig. 3b).  $\text{SiO}_2$  concentration also negatively

correlated with TOC (Fig. 3c), suggesting that Si was mainly from terrigenous clastic material and the content of authigenic diatom was very low. A discrimination diagram of  $\log(\text{SiO}_2/\text{Al}_2\text{O}_3) - \log(\text{TiFe}_2\text{O}_3/\text{K}_2\text{O})$  can provide accurate classification of rocks. From Fig. 3d, oil shale samples mainly plotted in shale and Fe-shale ranges.

### 4.2.2 Rare earth element characteristics

Total REEs ( $\Sigma\text{REE}$ ) of oil shale samples were relatively low (138.51–228.66 ppm, Table 2) with a high ratio (7.05–11.71) of light REEs (LREEs) to heavy REEs (HREEs) (L/H). High L/H ratio indicates a relative enrichment of LREEs and deficit of HREEs. After normalization to North American Shale Composite (NASC) (167.41  $\mu\text{g/g}$ ; Haskin et al. 1968), the REE distribution pattern showed a flat LREE trend and horizontal or slightly left-leaning HREE trend with inconspicuous negative Ce anomaly ( $\delta\text{Ce} = 0.89$ –1.02, averaging 0.94) and positive Eu anomaly ( $\delta\text{Eu} = 0.70$ –1.41, averaging 1.11) (Fig. 4a; Table 2). In addition, HREEs showed a slightly rich trend, influenced by the absorption of organic matter (Fig. 4a) (Tu and Xu 2016).

### 4.2.3 Trace element characteristics

Selected trace elements are shown in Table 3. The characteristics of trace elements in oil shale samples can be quantitatively depicted by enrichment factor (EF), defined as the ratio of the concentration to the corresponding value of upper continental crust (UCC) (Taylor and McLennan 1985). The EFs of these elements varied and were classified into three types: (1) Enrichment type (average EF > 1.1): Ba, Cu, Zn, Pb, Th, and U; (2) Equal type (average EF = 1 ± 0.1): Co; and (3) Deficit type (average EF < 0.9): Sr and Ni (Fig. 4b;

**Table 3** Trace elements and related parameters of oil shale samples (trace elements in ppm)

Sample no.	Sr	Ba	Cu	Zn	Pb	Th	U	Co	Ni	Cu + Pb + Zn	Sr/Ba	Fe/Ti	(Mn + Fe)/Ti	U/Th	$\delta\text{U}$
ZK702H6	110.40	380.90	90.30	98.00	51.90	22.20	28.50	13.30	22.00	240.20	0.29	27.96	28.36	1.28	1.59
ZK702H14	162.00	515.70	139.20	117.90	45.90	14.90	54.10	21.60	34.20	303.00	0.31	30.68	30.85	3.63	1.83
ZK702H18	229.80	463.40	144.50	107.00	35.40	10.80	61.30	15.10	29.10	286.90	0.50	30.72	30.94	5.68	1.89
ZK702H24	384.90	774.60	142.10	116.70	47.00	9.56	61.10	14.60	26.90	305.80	0.50	31.29	31.56	6.39	1.90
ZK702H32	328.20	792.60	132.30	122.10	37.90	12.70	47.00	14.70	28.30	292.30	0.41	33.01	33.35	3.70	1.83
ZK1501H3	185.00	562.40	139.30	99.80	43.80	15.80	68.20	15.80	27.70	282.90	0.33	28.63	28.99	4.32	1.86
ZK1501H6	151.70	438.50	150.10	101.20	47.70	12.60	61.70	18.90	31.20	299.00	0.35	37.57	37.86	4.90	1.87
ZK1501H11	438.80	765.10	141.90	121.90	48.00	9.96	51.10	17.70	30.00	311.80	0.57	25.59	26.19	5.13	1.88
ZK1501H13	436.80	631.70	49.40	69.70	33.70	19.60	20.00	12.00	17.40	152.80	0.69	15.22	15.53	1.02	1.51
ZK1501H15	425.00	849.80	123.10	117.80	52.80	15.10	47.30	17.40	31.00	293.70	0.50	23.84	24.67	3.13	1.81
ZK1501H17	375.80	838.90	30.90	77.10	30.30	11.60	6.82	8.57	14.70	138.30	0.45	11.12	11.45	0.59	1.28
ZK2709H1	160.50	513.60	41.00	120.70	42.50	17.60	4.21	15.90	37.00	204.20	0.31	11.03	11.42	0.24	0.84
ZK2709H3	192.40	649.50	97.50	100.50	31.90	13.10	17.70	17.80	36.80	229.90	0.30	18.37	18.85	1.35	1.60
ZK2709H5	236.10	680.40	31.20	74.90	32.80	16.60	6.41	7.93	20.10	138.90	0.35	10.03	10.46	0.39	1.07
ZK2709H6	182.00	612.00	95.90	95.10	29.70	12.00	21.60	17.50	36.90	220.70	0.30	16.74	17.21	1.80	1.69
ZK2709H8	177.70	662.00	64.20	101.00	33.60	14.00	12.70	17.10	36.70	198.80	0.27	14.09	14.42	0.91	1.46
ZK2709H11	159.30	692.70	66.60	102.50	35.80	14.40	12.40	18.30	40.70	204.90	0.23	14.42	14.70	0.86	1.44
ZK2709H12	245.50	635.40	40.10	105.00	31.10	12.10	2.94	15.80	41.00	176.20	0.39	8.68	8.77	0.24	0.84
ZK719H7	133.30	486.20	42.40	90.90	27.20	14.50	5.90	14.80	33.00	160.50	0.27	13.05	13.34	0.41	1.10
ZK719H13	155.40	584.00	53.20	96.80	31.30	15.00	14.00	15.50	37.30	181.30	0.27	13.42	13.78	0.93	1.47
ZK719H16	205.00	540.00	43.00	101.00	30.40	14.60	3.07	16.70	34.00	174.40	0.38	9.81	9.97	0.21	0.77
Average	241.70	622.35	88.49	101.79	38.13	14.22	28.95	15.57	30.76	228.40	0.38	20.25	20.60	2.24	1.50
UCC <sup>a</sup>	350.00	550.00	25.00	71.00	17.00	10.70	2.80	17.00	44.00	113.00	0.64	8.85	9.00	0.26	0.88

<sup>a</sup> Data cited are from Taylor and MacLennan (1985)

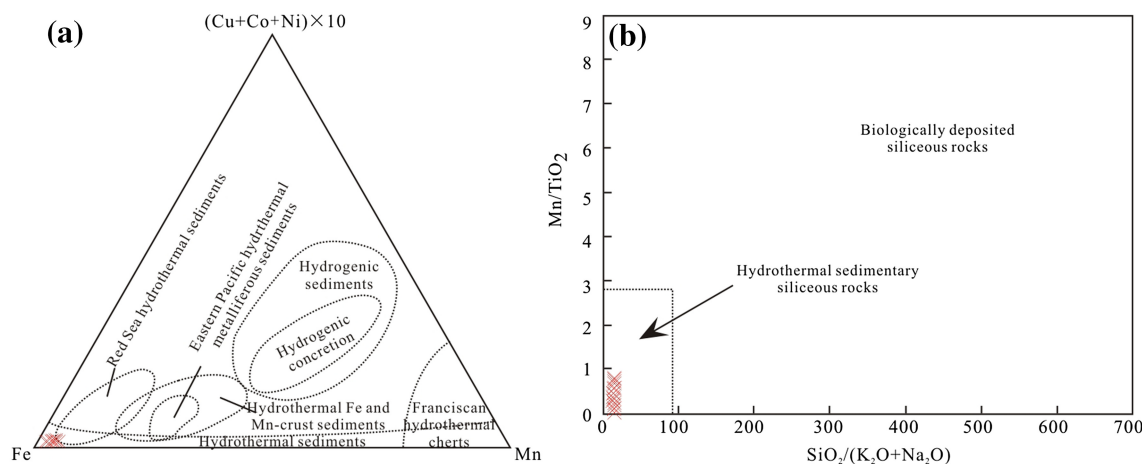


**Fig. 5** **a** Ternary diagram discrimination of oil shale samples and the base map is from Qi et al. (2004) and He et al. (2016), **b** genesis discrimination diagram of oil shale samples and the base map is from Li et al. (2014) and He et al. (2016)

Table 3). A discrepancy in enrichment level of trace elements is associated with a paleo-sedimentation environment.

## 5 Discussion

### 5.1 Evidence of hydrothermal fluid activity

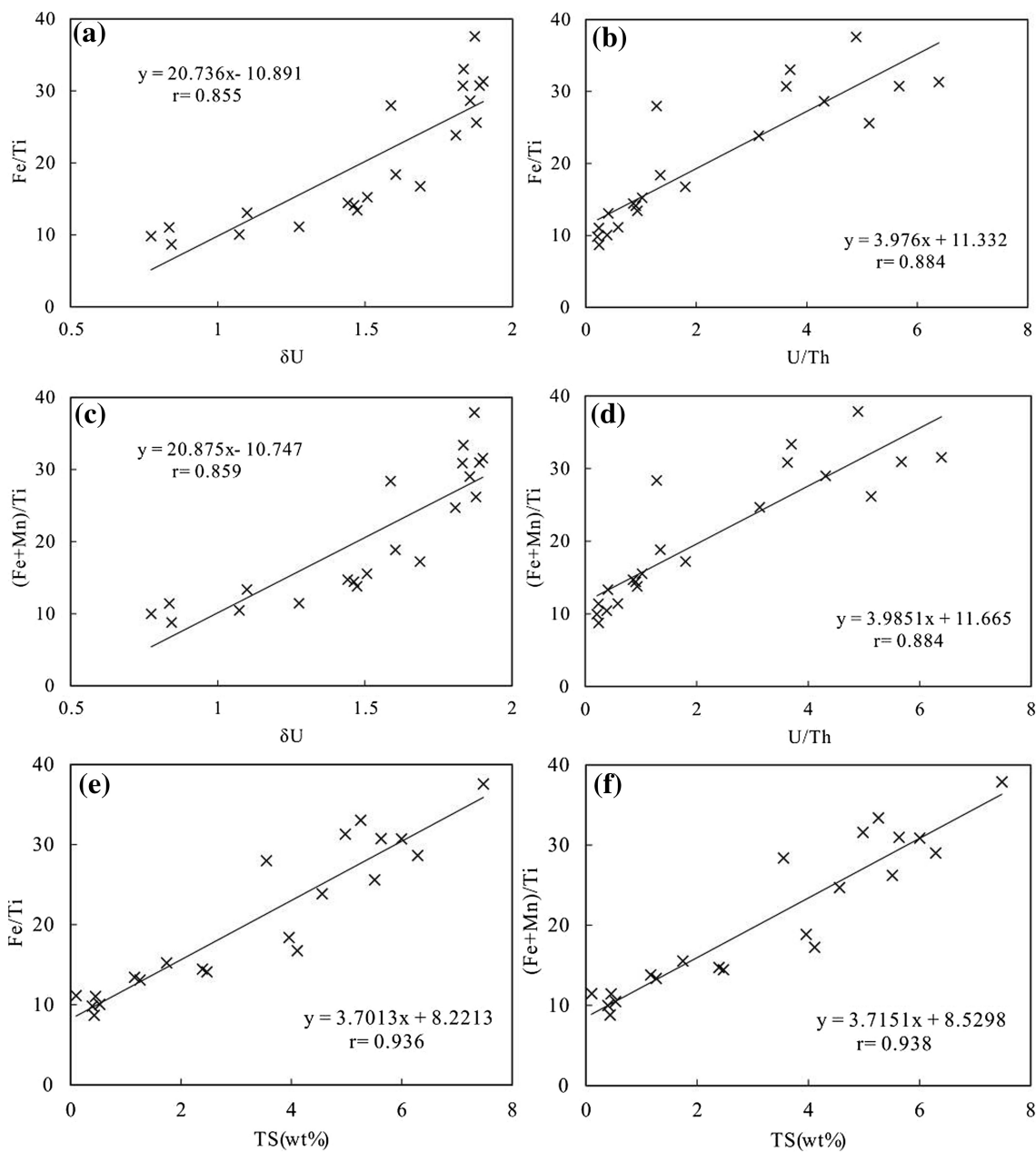
REEs in hydrothermal sedimentation have been widely studied (Rona et al. 1983; Zhang et al. 2003; Jia et al. 2016) and can be used to identify hydrothermal fluid activity. Generally, after being normalized to NASC (Taylor and McLennan 1985), a positive Eu anomaly is a signature of hydrothermal fluid (Zhang et al. 2003; Jia et al. 2016). As discussed above,  $\delta\text{Eu}$  of oil shale samples showed positive anomalies (with the exception of ZK702H6), implying hydrothermal fluid activity during oil shale sedimentation. A negative anomaly of Ce can also indicate hydrothermal fluid in sediments (Jia et al. 2016). The  $\delta\text{Ce}$  of most oil shale samples showed negative anomaly (with the exception of ZK2709H12), suggesting the influence of hydrothermal fluid. In distribution pattern of REEs (Fig. 4a), a slightly enriched trend of HREEs is generally associated with hydrothermal fluid activity (Jia et al. 2016). In addition, some discrimination diagrams of trace elements and major elements can also indicate hydrothermal activity. The diagrams of Fe versus Mn versus  $(\text{Cu} + \text{Co} + \text{Ni}) \times 10$  and  $\text{SiO}_2/(\text{K}_2\text{O} + \text{Na}_2\text{O})$  versus  $\text{MnO}/\text{TiO}_2$  clearly manifest hydrothermal fluid activity (Fig. 5a, b).  $\text{Fe}/\text{Ti}$  and  $(\text{Fe} + \text{Mn})/\text{Ti}$  can indicate the intensity of hydrothermal input (Chu et al. 2016). Values of more than 20 and 15, respectively, are regarded as indicative of hydrothermal input and the intensity gradually increases with increasing values. The corresponding average values of oil shale samples were 20.25 and 20.60,

respectively, suggesting the Chang 7 oil shale in the southern Ordos Basin was affected by hydrothermal fluid activity.

### 5.2 Influence of hydrothermal fluid activity on paleo-environment

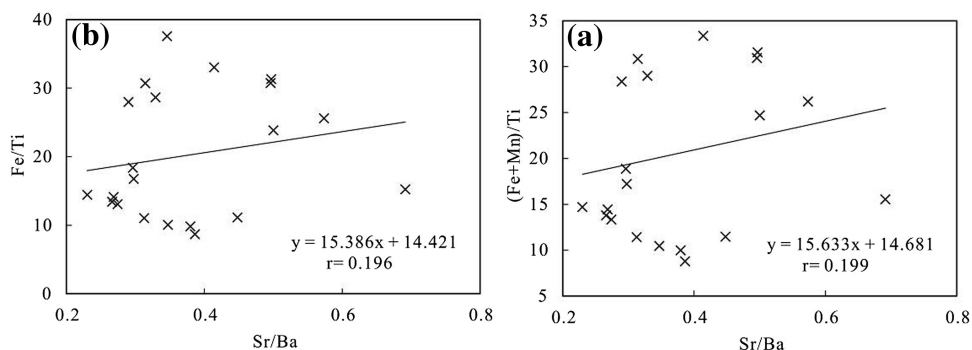
In discussing the impact on hydrothermal intensity on redox conditions, two parameters— $\delta\text{U}$  [ $\delta\text{U} = 2\text{U}/(\text{U} + \text{Th}/3)$ ] and  $\text{U}/\text{Th}$ —are quoted to represent redox degree (Ernst et al. 1970; Deng and Qian 1993; Jones and Manning 1994; Teng et al. 2004, 2005; Tribouillard et al. 2006; Zhao et al. 2016). Generally,  $\delta\text{U}$  and  $\text{U}/\text{Th}$  indicate an oxidizing environment when they are <1 and 0.75, respectively, and reducing conditions when they are more than 1 and 1.25, respectively. With an increasingly reducing environment, these two parameters increase. The average values of  $\delta\text{U}$  and  $\text{U}/\text{Th}$  of oil shale samples were 1.50 and 2.24, respectively, indicating that the environment during oil shale sedimentation was dominated by reducing conditions.

Hydrothermal fluid not only provides thermal energy but also plenty of reducing gas ( $\text{H}_2$ ,  $\text{CH}_4$ ,  $\text{CO}$ , and  $\text{H}_2\text{S}$ ) (Chen and Sun 2004; Zhang et al. 2010). The reducing gas can consume lots of oxygen and change physiochemistry, leading to reducing conditions. This can be demonstrated with diagrams of  $\text{Fe}/\text{Ti}$  and  $(\text{Fe} + \text{Mn})/\text{Ti}$  versus  $\delta\text{U}$  and  $\text{U}/\text{Th}$ . In oil shale samples,  $\text{Fe}/\text{Ti}$  and  $(\text{Fe} + \text{Mn})/\text{Ti}$  showed high positive correlation of  $\delta\text{U}$  and  $\text{U}/\text{Th}$  (correlation coefficients ranging from 0.855 to 0.884) (Fig. 6a–d), which means that reducing conditions increased with growing intensity of hydrothermal fluid activity. TS concentration is associated with redox conditions and a high content of TS usually indicates reducing conditions, while a low TS content points to an oxidizing environment.



**Fig. 6** Correlation diagrams of Fe/Ti and (Fe + Mn)/Ti with  $\delta$ U, U/Th and TS concentration in oil shale samples

**Fig. 7** Correlation diagrams of Sr/Ba with Fe/Ti and (Fe + Mn)/Ti in oil shale samples



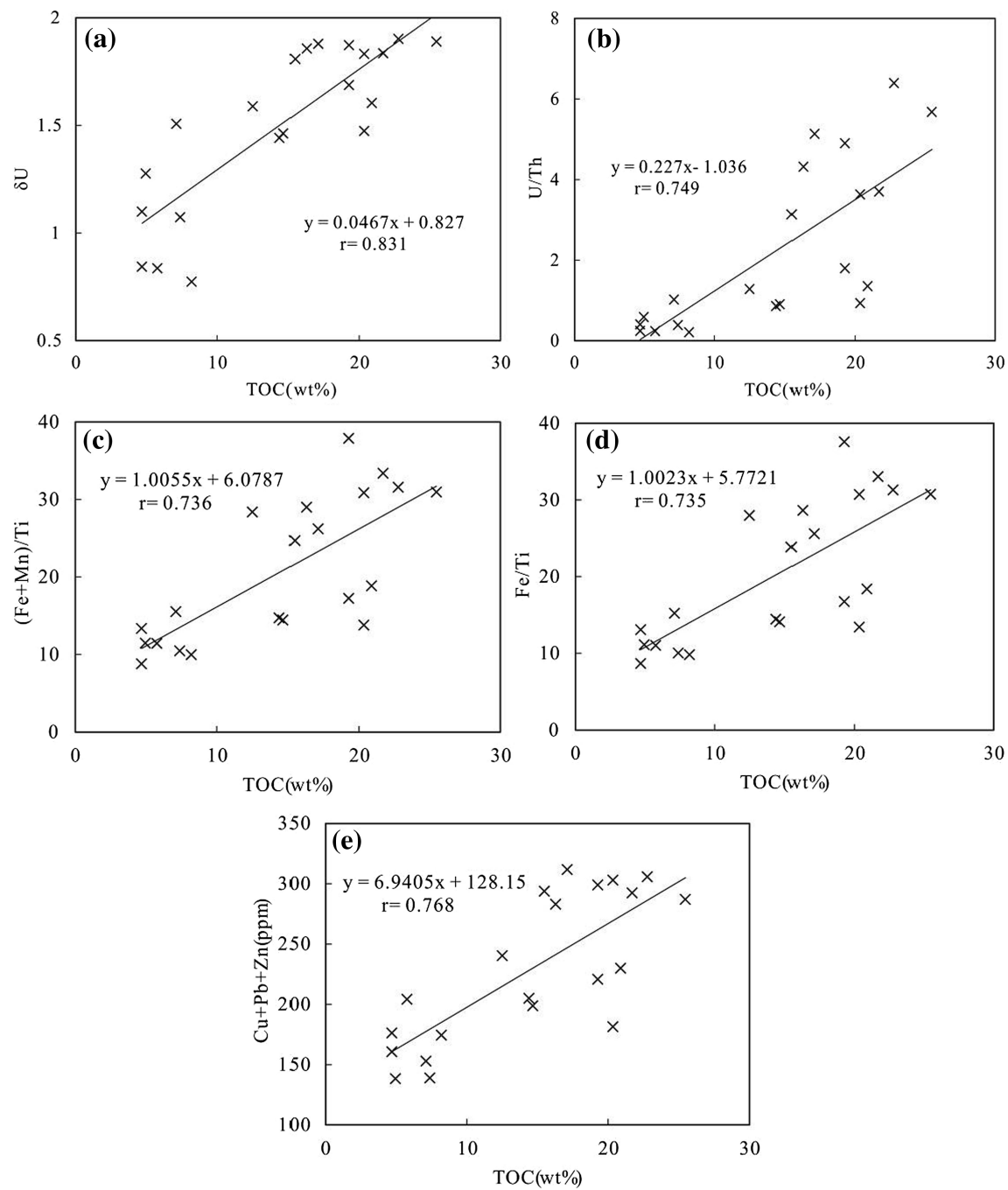


**Fig. 8** Correlation diagrams of TOC with  $\delta\text{U}$ ,  $\text{U}/\text{Th}$ ,  $(\text{Fe} + \text{Mn})/\text{Ti}$ ,  $\text{Fe}/\text{Ti}$  and  $\text{Cu} + \text{Pb} + \text{Zn}$  concentration

(Hakimi et al. 2016). The extreme high positive correlations between TS concentration and  $\text{Fe}/\text{Ti}$  ( $r = 0.936$ ) and  $(\text{Fe} + \text{Mn})/\text{Ti}$  ( $r = 0.938$ ) further indicates that hydrothermal fluid activity made an important contribution to reducing conditions in this case (Fig. 6e–f).

Due to the huge difference between Sr and Ba in supergene environments, Ba is more easily deposited in salt water than is Sr. Thus, Sr/Ba can be a sensitive indicator of paleosalinity (Wang et al. 1979, 2014a, b; Wang and Wu

1983; Li and Chen 2003; Li et al. 2015). Sr/Ba ratios of <0.6, 0.6–1, and >1 denote fresh, brackish, and salt water environments, respectively. The Sr/Ba of oil shale samples ranged from 0.23 to 0.69, averaging 0.38, suggesting mainly fresh water sedimentation. Sr/Ba of samples showed low correlation coefficients with  $\text{Fe}/\text{Ti}$  ( $r = 0.196$ ) and  $(\text{Fe} + \text{Mn})/\text{Ti}$  ( $r = 0.199$ ), indicating that hydrothermal fluid activity had a negligible impact on paleosalinity (Fig. 7a, b).

### 5.3 Influence on organic matter from hydrothermal fluid activity

Hydrothermal fluid activity can facilitate convection and circulation, thus exchanging nutritional ingredients. Some abundant life nutrition elements (P, N, Cu, Fe, Mo, and V) associated with hydrothermal fluid can improve productivity (Zhang et al. 2010; He et al. 2016), encouraging production of organic matter. Reducing conditions induced by hydrothermal fluid activity directly determine the preservation condition of organic matter.  $\delta\text{U}$  and U/Th both showed a positive relationship with TOC concentration (Fig. 8a, b), suggesting that, on one hand, reducing conditions contribute to organic preservation, while on the other hand, hydrothermal fluid activity affects not only the enrichment of organic matter, but also its preservation.

In oil samples, TOC concentration showed positive correlations with Fe/Ti and (Fe + Mn)/Ti, suggesting that hydrothermal fluid has a positive influence on organic matter (Fig. 8c, d). Meanwhile, hydrothermal fluid can change salinity. Low-salinity water can also support organic matter preservation.

Previous studies have demonstrated that Cu, Pb, and Zn are the typical sulfophilic elements (Chen et al. 2004). The enrichment of these three elements is controlled by hydrothermal fluid activity and terrestrial input. In general, the degree of enrichment is positively associated with the intensity of hydrothermal fluid activity (Chen et al. 2004). The positive correlation ( $r = 0.768$ ) between Cu + Pb + Zn and TOC concentration further supports this (Fig. 8e).

Therefore, the strengthening intensity of hydrothermal fluid activity would be conducive to formation and preservation of organic matter in the lacustrine environment.

## 6 Conclusions

There is a clear positive correlation between hydrothermal fluid activity and the formation and preservation of lacustrine superior source rocks based on elemental geochemistry. We conclude:

- (1) Oil yield, TOC, and TS of oil shale of Chang 7 oil layer from the southern Ordos Basin ranged from 1.4 wt% to 9.1 wt%, 4.69 wt%–25.48 wt%, and 0.10 wt%–7.48 wt%, respectively. Sulfur in oil shale was mainly organic sulfur, influenced by organic matter.
- (2) Major elements in oil shale consisted mainly of SiO<sub>2</sub>, Al<sub>2</sub>O<sub>3</sub>, and TFe<sub>2</sub>O<sub>3</sub>; based on the Al/Si ratio, the main mineral was quartz. A log(SiO<sub>2</sub>/Al<sub>2</sub>O<sub>3</sub>)–log(TFe<sub>2</sub>O<sub>3</sub>/

K<sub>2</sub>O) discrimination diagram revealed that the oil shale was dominated by shale and Fe-shale. Si/(Si + Al + Fe) demonstrated that the depositional environment was not far from a terrigenous provenance.

- (3) The distribution pattern of REEs, combined with  $\delta\text{Eu}$ ,  $\delta\text{Ce}$ , and diagrams of Fe versus Mn versus (Cu + Co + Ni) × 10 and SiO<sub>2</sub>/(K<sub>2</sub>O + Na<sub>2</sub>O) versus MnO/TiO<sub>2</sub> suggest that hydrothermal fluids were present during oil shale sedimentation. The intensity indicators of hydrothermal fluid activity, Fe/Ti and (Fe + Mn)/Ti, also support this conclusion.
- (4)  $\delta\text{U}$  and U/Th of oil shale samples indicate reducing conditions during oil shale sedimentation. Sr/Ba ratios indicated that oil shale was deposited in fresh water. The high correlation coefficients of Fe/Ti and (Fe + Mn)/Ti with  $\delta\text{U}$ , U/Th, and TS clearly manifested the positive contribution by hydrothermal fluid activity on reducing conditions. Sr/Ba showed low correlation with Fe/Ti and (Fe + Mn)/Ti, implying that hydrothermal fluid activity had little impact on paleosalinity.
- (5) Fe/Ti, (Fe + Mn)/Ti,  $\delta\text{U}$ , U/Th, and Cu + Pb + Zn were highly positively correlated with TOC in oil shale samples, suggesting that the strengthening intensity of hydrothermal fluid activity is beneficial to the formation and preservation of organic matter.

**Acknowledgements** This work was supported with funding from the National Natural Science Foundation of China (No. 41173055) and the Fundamental Research Funds for the Central Universities (No. 310827172101).

## References

- Bischoff JL (1969) Red Sea geothermal brine deposits: their mineralogy, chemistry, and genesis. Hot Brines and Recent Heavy Metal Deposits in the Red Sea. Springer, Berlin
- Chen JF, Sun XL (2004) Preliminary study of geochemical characteristics and formation of organic matter rich stratigraphy of Xiamaling-Formation of later proterozoic in North China. Nat Gas Geosci 15(2):110–114 (in Chinese with English Abstract)
- Chen JF, Sun XL, Liu WH, Zheng JJ (2004) Geochemical characteristics of organic matter-rich strata of lower Cambrian in Tarim Basin and its origin. Sci China Ser D Earth Sci 34(S1):107–113 (in Chinese with English Abstract)
- Chu CL, Chen QL, Zhang B, Shi Z, Jiang HJ, Yang X (2016) Influence on formation of Yuertusi source rock by hydrothermal activities at Dongergou section, Tarim Basin. Acta Sedimentol Sin 34(4):803–810 (in Chinese with English Abstract)
- Deng HW, Qian K (1993) Sedimentary geochemistry and environmental analysis. Gansu Science and Technology Press, Lanzhou (in Chinese)
- Ernst TW (1970) Geochemical facies analysis. Elsevier, Amsterdam

- Fu X, Wang J, Zeng Y, Tan F, Chen W, Feng X (2010a) Geochemistry of rare earth elements in marine oil shale—a case study from the Bilong Co area, Northern Tibet, China. *Oil Shale* 27(3):194–208
- Fu X, Wang J, Zeng Y, Tan F, Feng X (2010b) REE geochemistry of marine oil shale from the Changshe Mountain area, Northern Tibet, China. *Int J Coal Geol* 81(3):191–199
- GB/T 14506.1 ~ 14-2010. Methods for chemical analysis of silicate rocks (in Chinese with English abstract)
- GB/T 14506.30-2010 Methods for chemical analysis of silicate rocks—part 30: determination of 44 elements (in Chinese with English abstract)
- GB/T 6730.17-2014 Iron ores—determination of sulfur content—combustion iodometric method (in Chinese with English abstract)
- Hakimi MH, Wan HA, Alqudah M, Makeen YM, Mustapha KA (2016) Organic geochemical and petrographic characteristics of the oil shales in the Lajjun area, Central Jordan: origin of organic matter input and preservation conditions. *Fuel* 181:34–45
- Haskin LA, Haskin MA, Frey FA, Wildeman TR (1968) Relative and absolute terrestrial abundances of the rare earths. *Orig Distrib Elem* 72:889–912
- He ZX (2003) Evolution history and petroleum of the Ordos Basin. Petroleum Industry Press, Beijing (in Chinese)
- He C, Ji L, Wu Y, Su A, Zhang M (2016) Characteristics of hydrothermal sedimentation process in the Yanchang formation, South Ordos Basin, China: evidence from element geochemistry. *Sed Geol* 345:33–41
- He C, Ji LM, Su A, Liu Y, Li JF, Wu YD, Zhang MZ (2017) Relationship between hydrothermal sedimentation process and source rock development in the Yanchang Formation, southern Ordos Basin. *Earth Sci Front*. doi:10.13745/j.esf.yx.2016-11-29
- Jia ZB, Hou DJ, Sun DQ, Huang YX (2016) Hydrothermal sedimentary discrimination criteria and its coupling relationship with the source rocks. *Nat Gas Geosci* 27(6):1025–1034 (in Chinese with English Abstract)
- Jones B, Manning DAC (1994) Comparison of geochemical indices used for the interpretation of depositional environments in ancient mudstones. *Chem Geol* 111(1–4):112–129
- Lai XD, Yang XY, Gao P, Wu BL, Liu CY, Sun WD (2010) Geochemical study on U-rich tuffs in Yanchang Group in the southern Ordos Basin: implications to their forming mechanism. *Chin J Geol* 45(3):757–776 (in Chinese with English Abstract)
- Li JL, Chen DJ (2003) Summary of quantified research method on paleosalinity. *Petrol Geol Recover Effic* 10(5):1–3 (in Chinese with English abstract)
- Li HZ, Zhai MG, Zhang LC, Gao L, Yang ZJ, Zhou YZ, He JG, Liang J, Zhou LY, Voudouris PC (2014) Distribution, microfabric, and geochemical characteristics of siliceous rocks in central orogenic belt, China: implications for a hydrothermal sedimentation model. *Sci World J* 4:1–25
- Li ZC, Li WH, Lai SC, Li YX, Li YH, Shang T (2015) The Palaeosalinity Analysis of Paleogene Lutite in Weihe Basin. *Acta Sedimentol Sin* 33(3):480–485 (in Chinese with English abstract)
- Li DL, Li RX, Wang BP, Liu Z, Wu XL, Liu FT, Zhao BS, Cheng JH, Kang WB (2016) Study on oil-source correlation by analyzing organic geochemistry characteristics: a case study of the Upper Triassic Yanchang Formation in the south of Ordos Basin, China. *Acta Geochim* 35(4):408–420
- Liu XW, Wang XF, Shi BG, Wang ZD, Yang X, Zheng JJ, Liu CY (2010) Influence of abnormal geothermal on hydrocarbon generation: case study on the diabase intrusion of the Santanghu Basin. *Acta Sedimentol Sin* 29(4):809–814 (in Chinese with English Abstract)
- Liu XJ, Liu YQ, Zhou DW, Li H, Cheng XH, Nan Y (2013) Deep fluid tracer in Ordos Basin: characteristics and origin of high natural gamma sandstone in Triassic Yanchang formation. *Earth Sci Front* 20(5):149–165 (in Chinese with English Abstract)
- Qi HW, Hu RZ, Su WC, Qi L, Feng JY (2004) Continental hydrothermal sedimentary siliceous rock and genesis of super-large germanium (Ge) deposit hosted in coal: a study from the Lincang Ge deposit, Yunnan, China. *Sci China Ser D Earth Sci* 47:973–984
- Qi FC, Li ZX, Zhang ZL, Wang WQ, Yang ZQ, Zhang Y (2015) Hydrothermal decarburization and uranium-polymetallic ore-mineralization in marine phosphorite, northwestern. *Earth Sci Front Hum* 22(4):188–199 (in Chinese with English Abstract)
- Qiu XW, Liu CY, Li YH, Mao GZ, Wang JQ (2009) Distribution characteristics and geological significances of Tuff interlayers in Yanchang formation of Ordos Basin. *Acta Sedimentol Sin* 27(6):1138–1146 (in Chinese with English abstract)
- Qiu XW, Liu CY, Mao GZ, Wu BS (2011) Petrological-Geochemical Characteristics of Volcanic Ash Sediments in Yanchang Formation in Ordos Basin. *Earth Science-Journal of China University of Geosciences* 36(1):139–150 (in Chinese with English Abstract)
- Qiu X, Liu C, Mao G, Deng Y, Wang F, Wang J (2014) Late Triassic tuff intervals in the Ordos basin, Central China: their depositional, petrographic, geochemical characteristics and regional implications. *J Asian Earth Sci* 80:148–160
- Qiu X, Liu C, Mao G, Deng Y, Wang F, Wang J (2015) Major, trace and platinum-group element geochemistry of the upper triassic nonmarine hot shales in the Ordos Basin, central China. *Appl Geochem* 53:42–52
- Rona PA, Bostrom K, Laubier L, Smith KL (1983) Hydrothermal Processes at Sea floor Spreading Centers. Springer, US, New York
- SH/T 0508-1992 The test method for oil yield from oil shale-The method of low temperature carbonization (in Chinese with English abstract)
- Sun XL, Chen JF, Liu WH, Zhang SC, Wang DR (2003) Hydrothermal venting on the seafloor and formation of organic-rich sediments—evidence from the Neoproterozoic Xiamaling formation, North China. *Geological Rev* 49(6):588–595 (in Chinese with English Abstract)
- Sun XL, Chen JF, Liu WH, Wang DR (2004) Geochemical characteristics of cherts of Lower Cambrian in the Tarim Basin and its implication for environment. *Petroleum Exploration and Development* 31(3):45–48 (in Chinese with English Abstract)
- Sun SS, Liu RH, Bai WH (2011) Effect Factor Analysis of Oil Content of Upper Triassic Oil Shale in Tongchuan Area. *Ordos Basin. China Petroleum Exploration* 16(2):79–83 (in Chinese with English Abstract)
- Taylor SR, McLennan SM (1985) The continental crust: its composition and evolution, an examination of the geochemical record preserved in sedimentary rocks. Blackwell, Palo Alto, p 312
- Teng GE, Liu WH, Xu Y, Chen JF (2004) Identification of effective source rocks of Ordovician marine sediments in Ordos Basin. *Prog Nat Sci* 14(11):1249–1252 (in Chinese)
- Teng GE, Hui LW, Xu YC, Chen JF (2005) Correlative study on parameters of inorganic geochemistry and hydrocarbon source rocks formative environment. *Adv Earth Sci* 20(2):193–200 (in Chinese with English Abstract)
- Tribouillard N, Algeo TJ, Lyons T, Riboulleau A (2006) Trace metals as paleoredox and paleoproduction proxies—An update. *Chem Geol* 232(1–2):12–32
- Tu QJ, Xu SQ (2016) The REE geochemistry of the Luogou formation in the Southern Junggar Basin and analysis of parent rock and tectonic setting in sediment-source region. *Xin Jiang Geol* 34(3):345–349 (in Chinese with English Abstract)
- Wang SM (2011) Ordos basin tectonic evolution and structural control of coal. *Geological Bull China* 30(4):544–552 (in Chinese with English Abstract)

- Wang YY, Wu P (1983) Geochemical criteria of sediments in the coastal area of Jiangsu and Zhejiang Provinces. *J Tongji Univ Nat Sci* 4:82–90 (in Chinese with English abstract)
- Wang YY, Guo WY, Zhang GD (1979) Application of some geochemical indicators in determining of sedimentary environment of the funing group (Paleogene), Jin-Hu depression, Kiangsu Provience. *J Tongji Univ* 7(2):51–60 (in Chinese with English abstract)
- Wang CY, Zheng RC, Liu Z, Liang XW, Li TY, Zhang JW, Li YN (2014a) Paleosalinity of chang 9 reservoir in longdong area, Ordos Basin and its geological significance. *Acta Sedimentol Sin* 32(1):159–165 (in Chinese with English abstract)
- Wang DY, Xin BS, Yang H, Fu JH, Yao JL, Zhang Y (2014b) Zircon SHRIMP U-Pb age and geological implications of tuff at the bottom of Chang -7 member of Yanchang Formation in the Ordos Basin. *Sci Chin Earth Sci* 44(10):2160–2171 (in Chinese with English Abstract)
- Wu FL, Li W, Li Y (2004) Delta sediments and evolution of the Yanchang formation of upper triassic in Ordos Basin. *J Palaeogeogr* 6:307–315 (in Chinese with English abstract)
- Xie XM, Teng GE, Qin JZ, Zhang QZ, Bian LZ, Yi LM (2015) Depositional environment, organisms components and source rock formation of siliceous rocks in the base of the Cambrian Niutitang Formation, Kaili, Guizhou. *Acta Geologica Sin* 89(2):425–439 (in Chinese with English Abstract)
- Yang JJ, Li KQ, Zhang DS (1992) Petroleum geology of China. Petroleum Industry Press, Beijing (in Chinese with English Abstract)
- Zeng ZG, Zhang W, Rong KB, Wang XY, Chen S, Cui LK, Jiang SL, Qi HY (2015) Seafloor hydrothermal activity and polymetallic sulfide resources potential in the East Pacific Rise. *Bull Mineral Petrol Geochem* 34(5):938–946 (in Chinese with English Abstract)
- Zhang WH, Jiang LJ, Gao H, Yang RD (2003) Study on sedimentary environment and origin of black siliceous rocks of the lower Cambrian in Giuzhou Province. *Bull Mineral Petrol Geochem* 22(2):174–178 (in Chinese with English Abstract)
- Zhang WZ, Yang H, Xie LQ, Yang YH (2010) Lake-bottom hydrothermal activities and their influences on the high-quality source rock development: a case from Chang 7 source rocks in Ordos Basin. *Pet Explor Dev* 37(4):424–429 (in Chinese with English Abstract)
- Zhang WZ, Yang H, Xie LQ, Xie GW (2011) Discovery of micro- and nannofossils in high grade hydrocarbon source rocks of the Triassic Yanchang Formation Chang 7 member in Ordos Basin and its scientific significance. *Acta Palaeontol Sin* 1:109–117 (in Chinese with English Abstract)
- Zhao J, Jin Z, Jin Z, Geng Y, Wen X, Yan C (2016) Applying sedimentary geochemical proxies for paleoenvironment interpretation of organic-rich shale deposition in the Sichuan Basin, China. *Int J Coal Geol* 163:52–71